A facile approach to durable, transparent and self-healing coatings with enhanced hardness based on Diels-Alder polymer networks

Giovanni Fortunato[a], Vincenzo Marroccoli[a], Francesca Corsini[a], Stefano Turri[a], and Gianmarco Griffini[a*]

[a]*Department of Chemistry, Materials and Chemical Engineering "Giulio Natta", Politecnico di Milano, Piazza Leonardo da Vinci 32, 20133 Milano, Italy.*

* Corresponding author *E-mail: gianmarco.griffini@polimi.it*

ABSTRACT

Prolonged durability in outdoor environment and ease of application are highly required features for self-healing coatings. To this end, a novel transparent and self-healing nanocomposite for optical applications, based on Diels-Alder (DA) chemistry is developed in this work. First, a novel, highly soluble, bismaleimide enabled a simple coating fabrication by coupling with furan-functionalized polyacrylates in industrially relevant solvents. The resulting crosslinked coatings exhibited high transparency and complete absence of color, as assessed by UV-vis spectroscopy. Their thermal behavior and the conditions required by the healing process were significantly affected by the degree of furan/maleimide functionality of the system. Secondly, the addition of a small amount of a commercial antioxidant stabilized the optical properties against photo-oxidative weathering, both on clear and titania-pigmented coatings, as determined by colorimetric analysis. Finally, dispersion of silica nanoparticles in the DA-based matrix allowed to enhance the surface hardness of the coatings, while retaining the self-healing ability.

KEYWORDS: self-healing, nanocomposites, acrylate, Diels-Alder, transparent coatings

1 Introduction

The development of functional coatings has been continuously driven by the need to impart properties like water repellence, corrosion protection or wear resistance to a wide variety of surfaces, ranging from basic tools to more advanced applications [1]. Specifically, in organic functional coatings the resin component, or binder, is the primary barrier against the environment (radiation, water, mechanical stress) and provides the adhesion to the substrate. A coating is continuously exposed to environmental agents during his service life, which results in degradation and mechanical damages. As a consequence, protective, aesthetic and functional properties are strongly reduced and ultimately lost [2]. This issue has recently raised the interest towards self-healing (functional) coatings, a class of smart materials able to repair small mechanical damages in response to a stimulus, which can be the damage event itself (autonomous mechanism) or an external trigger in the form of heat or radiation (non-autonomous mechanism) [3-7].

The latter approach is commonly referred to as intrinsic self-healing, as the material is specifically designed as a reversible polymer network, able to soften when a suitable stimulus is provided and to toughen when the stimulus is removed [8]. Among the different reversible interactions, dynamic covalent bonds stand out as they provide superior robustness in the design of self-healing materials, compared to hydrogen bonding or aromatic π-π stacking [9]. Many dynamic covalent chemistries, which have long been known as tools for organic synthesis, have been increasingly applied to polymer networks [10-12] to enable self-healing in addition to enhanced recyclability, moldability and, more generally, stimuli-responsiveness.

In this context, the Diels-Alder (DA) reaction is a paradigmatic example. DA is a click type cycloaddition between a diene and a dienophile, more commonly a furan and a maleimide, forming a cyclic adduct, which can be broken at higher temperatures through the retro Diels-Alder (r-DA) process. Thus, the adducts can act as thermally reversible crosslinks in a polymer network [13]. Since the discovery of DA reaction in 1942 [14], it took nearly forty years to understand its value as a tool for reversible crosslinking in polymers, starting from the patent by Craven [15] and the milestone

work of Wudl [16] on thermally remendable thermosets. Owing to its high efficiency and the availability of furan and maleimide precursors, DA thermal reversibility has been exploited in a wide variety of polymer matrices: most recent examples include epoxies [17-20], polyurethanes [21-23], elastomers [24-26], polyketones [27, 28] and polyesters [29, 30], mainly as bulk materials.

Conversely, DA-functional polyacrylates have been mostly designed for self-healing coatings [31-47]. Gandini [48] firstly reported a simple strategy to design DA-reversible, acrylate-based polymer networks, by simply combining linear copolymers of furfuryl methacrylate (FMA) with difunctional, maleimide linkers. The majority of the subsequent works on the topic followed the same approach [31-33, 35, 40, 44] and mainly focused on tuning thermal and self-healing properties by tailoring the network architecture through controlled radical polymerizations and/or by adjusting the amount of functional comonomer. A high healing ability, obtained by heating the scratched surface over 120 °C for several hours, is generally reported for these systems.

A major drawback of these approaches is the opaque and colored appearance of the reported systems typically resulting from the use of aromatic bismaleimide linkers, which limits the functionality of the proposed coatings only to their self-healing ability while hindering their use in optical applications where high levels of transmittance in the visible range are normally required. In a previous work from our group [49] a simple strategy towards the combination of DA-based self-healing ability with outstanding transparency in polyacrylate coatings was presented. Furan-functionalized polyacrylates synthetized *via* free radical polymerization of FMA and other alkyl methacrylates were crosslinked with aliphatic bismaleimides. The obtained coatings were colorless, highly transparent, and possessed excellent adhesive strength. Furthermore, thermal properties and wettability could be tuned by changing the type of alkyl methacrylate comonomer to meet the requirements for outdoor use.

However, the proposed system presents some clear technological limits. First, the previously used bismaleimide linkers need to undergo a thorough purification process to meet the strict transparency requirements demanded by optical applications. Secondly, their scarce solubility in common solvents for commercial coatings effectively limits their processability at large scale. Furthermore, no

information is available in the literature on the photo- and thermo-oxidative degradation behavior of DA-based functional acrylate coatings, notwithstanding the crucial role these aspects play when designing functional transparent coatings simultaneously exhibiting self-healing ability, prolonged outdoor durability and retention of excellent optical transparency over time.

In order to overcome these limitations, a novel aliphatic bismaleimide crosslinker with enhanced solubility was synthetized in high yield from biobased butanediol in a one-step procedure. Upon reaction of such aliphatic maleimide with linear copolymers of FMA and 2-ethylhexylmethacrylate (EHMA) with different degree of furan functionality, transparent and colorless DA-based coatings were obtained. The thermal reversibility of such reversibly crosslinked materials was assessed by differential scanning calorimetry (DSC) and solubility experiments. The effect of the extent of crosslinking on the thermal properties, wettability, and adhesion strength of the obtained coatings as well as on the threshold conditions to allow self-healing to occur was studied. The photo-oxidative durability and healing capability of these DA-based polymers upon accelerated weathering was assessed *via* Fourier-transform infrared (FTIR) and UV-Vis spectroscopy on clear and titania-pigmented coatings.

The incorporation of nanostructured materials into a polymer matrix is a valid method to impart novel functionalities like conductivity [50], magnetism [51] or enhance thermal [52] and mechanical properties [53, 54]. Within this context, transparent polymer coatings for optical applications are no exceptions[55], provided that the fillers do not impair their high transmittance. To this end, nanofillers should possess a refractive index closely matching the one of the matrix. At the same time, experimental parameters such as the filler content and the dispersion method must be carefully selected, in order to avoid formation of aggregates, which cause scattering and, eventually, loss of transparency [56]. Most commonly reported nanofillers for transparent nanocomposites include metals (Ag, Au), oxides (TiO_2, ZnO, modified tin oxides, SiO_2), sulfides (CdS, PbS) and clays [56, 57]. In particular silica nanoparticles (nano-SiO_2) are among the most used reinforcing fillers for coatings [58], as they provide scratch and impact resistance, improved thermal stability and good

barrier properties, while retaining the optical transparency at low filler content [59-63]. Based on these features, in this work (fumed) silica nanoparticles were incorporated into the DA-coating, in order to obtain self-healing transparent nanocomposites with increased surface hardness. The effect of the nanosilica content was then evaluated on the optical, mechanical and functional properties of the coatings.

To the best of our knowledge, this represents the first systematic investigation of the functional and technological properties of self-healable, transparent polyacrylate coatings based on reversible DA chemistry and their silica-based nanocomposites.

2 Experimental

2.1 Materials

Biobased 1,4-butanediol was kindly provided by Novaresine srl. 6-maleimido hexanoic acid (90%), sulfuric acid, furfuryl methacrylate (FMA), 2-ethylhexyl methacrylate (EHMA), sodium sulfate anhydrous, N,N-dimethylformamide (DMF), fumed silica (average size 7 nm) and titania were all purchased from Sigma-Aldrich. Irganox 1010 was supplied by BASF. Toluene, diethyl ether, tetrahydrofuran (THF), 2-butanone (MEK), chloroform and azobisisobutyronitrile (AIBN) were obtained from Fluka. Sodium bicarbonate was purchased from Solvay.

2.2 Synthesis of diester bismaleimide (DEBM)

The new diester bismaleimide of 1,4 butanediol (DEBM) was synthetized by suspending 1,4-butanediol (9 mmol), 6-maleimidohexanoic acid (18 mmol) and sulfuric acid (23 µL) in toluene (15 mL) in a three-necked round bottom flask equipped with a Dean-Stark trap, a rubber septum with a needle for nitrogen flushing and a magnetic stirrer. The mixture was slowly heated with an oil bath under inert atmosphere till reflux (130-135 °C). After 2 h of reflux, the trap containing toluene and formed water was emptied and additional 2.5 mL of toluene was distilled off. The reaction mixture was cooled to room temperature (rt), added with 5 mL of diethyl ether and washed with saturated aqueous solution of sodium bicarbonate (15 mL) and distilled water (15 mL). The organic phase was collected and dried over anhydrous sodium sulfate and filtered. After solvent removal under vacuum, a yellow viscous liquid was obtained that slowly turned to an off-white solid at rt. Yield = 70%; mp 45 °C; IR (KBr): ν (cm^{-1}) = 3100 (=C−H), 2950 (C−H), 1730 (C=O ester), 1700 (C=O maleimide), 1409 (C−N−C), 830 and 696 (maleimide ring).

^{1}H-NMR (400 MHz, $CDCl_3$, δ): 6.66 (s, 4H, $\underline{H}C=C\underline{H}$), 4.06 (m, 4H; $OC\underline{H}_2$), 3.51 (t, 4H, $NC\underline{H}_2$), 2.29 (t, 4H; $(CO)C\underline{H}_2$), 1.69 (m, 4H; $OCH_2C\underline{H}_2$),1.60 (m, 8H, $(CO)CH_2C\underline{H}_2$ and $NCH_2C\underline{H}_2$), 1.31 (m, 4H, $C\underline{H}_2$). Electrospray ionization MS (positive ion mode): calcd. for $C_{24}H_{32}N_2O_8$ $[M + Na]^+$: *m/z* = 449.19; found: 449.2.

2.3 Synthesis of poly(2-ethyl hexyl methacrylate-co-furfuryl methacrylate)

Copolymers of FMA and EHMA were prepared by free radical polymerization. In a typical experiment, a 25 wt. % chloroform solution of the two monomers, combined at different molar ratios, was charged into a three-necked round bottom flask, equipped with a reflux condenser and a magnetic stirrer. After nitrogen flushing for 30 min, the flask was sealed with rubber septa and heated by means of an oil bath up to 82 °C. Upon addition of freshly recrystallized AIBN (1 mol. % with respect to monomers) the reaction mixture was stirred for 4 h. The polymer was isolated after several precipitation steps in cold methanol and re-dissolution in chloroform. Transparent solids were obtained after solvent removal in vacuum (50 °C for 12 h).

2.4 Coating preparation

Co-polyacrylates with different degree of furan functionalization were dissolved in MEK and a stoichiometric amount of diester bismaleimide (DEBM) was added (1:1 molar ratio between furan and maleimide groups). The obtained solutions were spin coated on glass slides using a Laurell WS-400BZ-6NPP/LITE apparatus. Concentration of the dry solids and angular velocity were varied in order to obtain coatings with different thicknesses, ranging from 3 to 25 μm. Coated glasses were then heated for 30 min at 150 °C and slowly cooled to rt in order to ensure solvent removal and crosslinking.

2.5 Nanocomposite coating preparation

Fumed silica nanoparticles (in the range of 1-5 wt.% with respect to dry crosslinked polymer) were dispersed in a 10 wt. % MEK solution of the furan-polymer *via* ultrasonication using a Sonics VCX130 apparatus (3 h, 90% amplitude, pulsed mode). Upon addition of DEBM, dispersions were spin coated (300 rpm) on glass and subjected to the same thermal treatment as unfilled coatings.

2.6 Structural and thermal characterization

^{1}H NMR (400 MHz) spectra were recorded on a Bruker Avance 400 using deuterated chloroform as solvent. FTIR spectra were recorded using a Thermo Nicolet Nexus 670 instrument. Measurements

were performed on solid films deposited on KBr discs, recording 64 accumulated scans at a resolution of 2 cm^{-1}. Gel permeation chromatography (GPC) analyses were performed on an apparatus consisting in a Waters 515 HPLC pump (mobile phase, THF; flow rate, 1 mL/min, at 35 °C), three Styragel columns (models HR 4, HR 3, and HR 2) from Waters, and a refractive index detector Waters 2410. Samples were dissolved in THF at a concentration of 0.2 wt %. A calibration curve was prepared by using monodispersed fractions of polystyrene. Differential scanning calorimetry (DSC) analyses were performed with a DSC 823e Mettler-Toledo instrument, by applying the following thermal cycle: from 25 °C to 180 °C, from 180 °C to -50 °C, and from -50 °C to 180 °C; with a heating/cooling rate of 20 °C/min. Thermogravimetric analyses (TGA) were performed with a Q500 TGA system (TA Instruments) from rt to 800 °C at a scan rate of 10 °C/min in air atmosphere.

2.7 Optical characterization

UV–visible spectroscopy analyses were performed at rt on an Evolution 600 UV–vis spectrophotometer (Thermo Scientific) on solid films coated on glass slides. Relative reflectance was measured on a Jasco V-570 UV-Vis-NIR spectrophotometer equipped with an integrating sphere and a PTFE foil as reference. Refractive index of selected coatings was measured using a Filmetrics F20 thin film analyser in the wavelength range 400–800 nm and the BK7 reflection standard was used to calibrate the instrument in the contact stage mode. The sample was prepared by spin coating a solution of copolymer and bismaleimide on a silicon wafer substrate (600 nm thickness) followed by a similar thermal treatment as the one reported above for coatings.

2.8 Microscopy characterization

Optical micrographs were recorded through an Olympus BX-60 reflected-light optical microscope equipped with an Infinity 2 digital camera. Scanning electron microscopy (SEM) and energy dispersive X-ray (EDX) analyses were performed using a Zeiss Evo 50 EP SEM apparatus (acceleration voltage of 5.0 kV) on samples coated with a thin layer of gold. Atomic force microscopy (AFM) measurements were performed in air and at room temperature on a Keysight 5600LS AFM

apparatus. The morphological characterization was carried out in tapping mode with 256 samples/line, 0.50 line/s and 10–80 μm scan range.

2.9 Photochemical stability

Weathering tests were performed by continuously irradiating the DA-based coatings for > 500 h in a Solarbox 3000e weather-o-meter chamber (Cofomegra srl), equipped with a Xenon lamp and an outdoor filter (λ > 280 nm). The total irradiance applied was equal to 550 W/m^2 in the 300–800 nm range at a temperature of 40 °C and an average relative humidity of 25 %. Tests were performed on both clear and titania (TiO_2) pigmented coatings, added with an antioxidant additive (Irganox 1010, 0.2 wt. %). Pigmentation was performed by dispersing TiO_2 powder in the copolymer solution (60 wt. % with respect to dry content). Colorimetric analysis was performed on a Konica Minolta CM-2600d spectrophotometer, in order to analyze the macroscopic color and determine the Hunter whiteness index (WI_H) and the total color difference (ΔE) calculated from CIELAB color coordinates [64].

2.10 Adhesion and surface properties

Adhesion strength of the DA-based coatings on glass substrates were determined through a PosiTest AT-M Manual pull-off tester (DeFelsko) by measuring the pulling force needed to detach a 20 mm-diameter aluminium dolly glued to the crosslinked coatings by means of a two-component epoxy adhesive (Araldite 2011, curing cycle: 50 °C, 24 h). Wettability was studied in terms of static optical contact angle (OCA) measurements, which were performed with an OCA 20 (DataPhysics) equipped with a CCD photo-camera and with a 500 μL Hamilton syringe to dispense liquid droplets. Water and diiodomethane (DIM) were used as probe liquids. The surface energy of the coatings was calculated according the Owens-Wendt-Rabel-Kaelble (OWRK) method [65]. Pencil hardness of the coatings was tested according to the ASTM D 3363 standard [66]. Hardness grade was assigned according to the softest pencil which caused a visible marking on the surface of the coating.

3 Results and discussion

3.1 Synthesis and properties of a novel aliphatic bismaleimide crosslinker

The aliphatic bismaleimide crosslinker (DEBM) reported for the first time in this work was synthetized *via* a one-step, Fischer esterification of biobased 1,4-butanediol with two equivalents of 6-maleimidohexanoic acid (Scheme 1A).

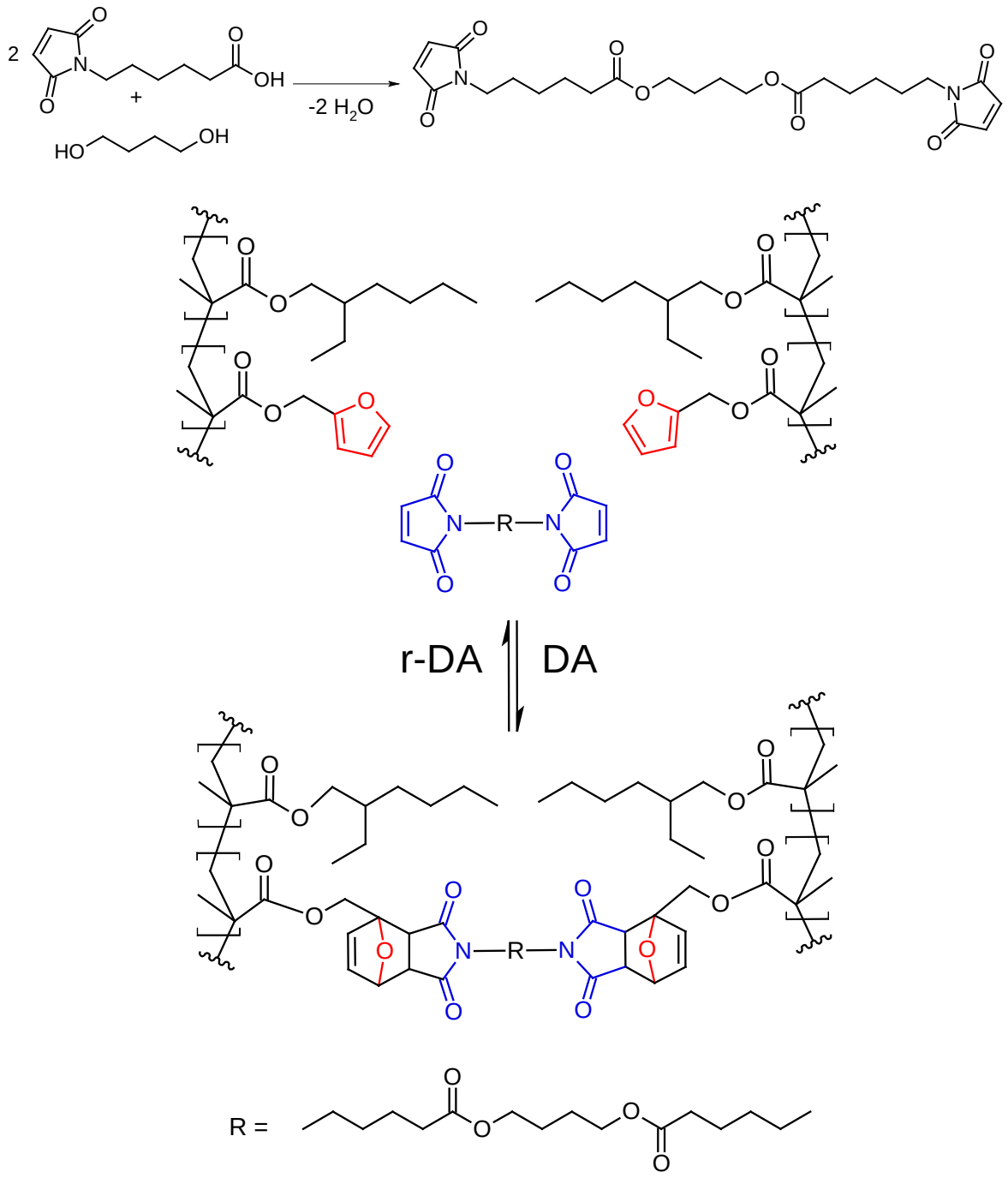

Scheme 1 (A) Synthesis of butanediol diester bismaleimide (DEBM) *via* esterification of 6-maleimidohexanoic acid with 1,4-butanediol; (B) Crosslinking and de-crosslinking of furan-functionalized polyacrylates (p-FMA-*co*-EHMA) via DA and r-DA reaction with the novel bismaleimide linker.

A common method for the synthesis of bismaleimides [67] entails the conversion of diamine precursors to maleamic acid, followed by a dehydration step. The reaction is characterized by the formation of dark colored byproducts, whose removal lowers the yield in the pure product [68]. Conversely, in the strategy presented here the maleimide moiety is already available in the acid precursor and, upon reaction with the diol, DEBM could be obtained in high yield and purity, as confirmed by ^{1}H-NMR, FTIR and mass spectra (see Experimental section and Figures S1, S2, S3 in the Supporting Information). Furthermore, differently from other aliphatic crosslinkers characterized by relatively high melting temperatures T_m such as those used in our previous study (1,6-bismaleimidohexane, T_m = 137 °C; 1,12-bismaleimidododecane, T_m = 112 °C) [49, 69], DEBM possesses a significantly lower melting point (45 °C) and exhibits excellent solubility in common solvents for industrial coatings like butyl acetate, ethyl acetate and MEK.

3.2 Synthesis and properties of furan-functionalized polyacrylates (p-FMA-co-EHMA)

A series of copolymers was obtained by free radical polymerization of FMA and EHMA combined at different molar ratios (see Table 1). Furan content, calculated from the ratio between the integrated signals at 4.9 (-OCH_2 protons of FMA) and 3.7 ppm (-OCH_2 protons of EHMA) in ^{1}H-NMR spectra (Figure S4 in the Supporting Information), was close to the targeted one. Polydispersity index (*Đ*) slightly increased with the furan content, as reported for similar systems, as a result of the occurrence of minor chain transfer reactions caused by the furan groups [48]. Owing to the random distribution of furfuryl and 2-(ethyl)hexyl groups, all polymers exhibited a single glass transition temperature (T_g) with T_g values ranging from -13 to 20 °C, as a function of furan groups content, consistently with prior literature [44, 48, 70].

Table 1 Reaction feed stoichiometry, composition, number average molecular weight (M_n), polydispersity ($Đ$) and thermal properties of linear copolymers of furfuryl and 2-(ethyl)hexyl methacrylate.

Sample	*FMA feed* [mol%]	*FMA* [a)] [mol%]	*Yield* [%]	M_n [b)] [kg/mol]	$Đ$ [b)]	T_g [c)] [°C]
FM10	10.0	9.9	72	51.1	1.82	-13
FM20	20.0	19.5	84	47.3	1.91	5
FM30	30.0	29.4	81	51.0	2.19	11
FM40	40.0	39.7	77	51.8	2.23	20

[a)] determined from ^{1}H-NMR; [b)] from GPC analyses; [c)] from DSC

3.3 Characterization of coatings crosslinked through DA chemistry

MEK solutions of furan-modified polyacrylates and DEBM, combined in 1:1 ratio between furan and maleimide groups, were visually transparent and colorless. Solid thin films were obtained upon deposition on glass slides by spin coating and thermal treatment (30 min at 150 °C followed by slow cooling to rt). Samples were coded as *FMxBM*, where *x* is the percent molar content of FMA in the linear polyacrylate (from 10 to 40) and *BM* refers to presence of DEBM crosslinker.

Crosslinking of furan-acrylates/bismaleimide networks was assessed through FTIR analysis. In Figure 1 spectra of representative sample *FM40BM*, recorded before and after the thermal treatment, are reported.

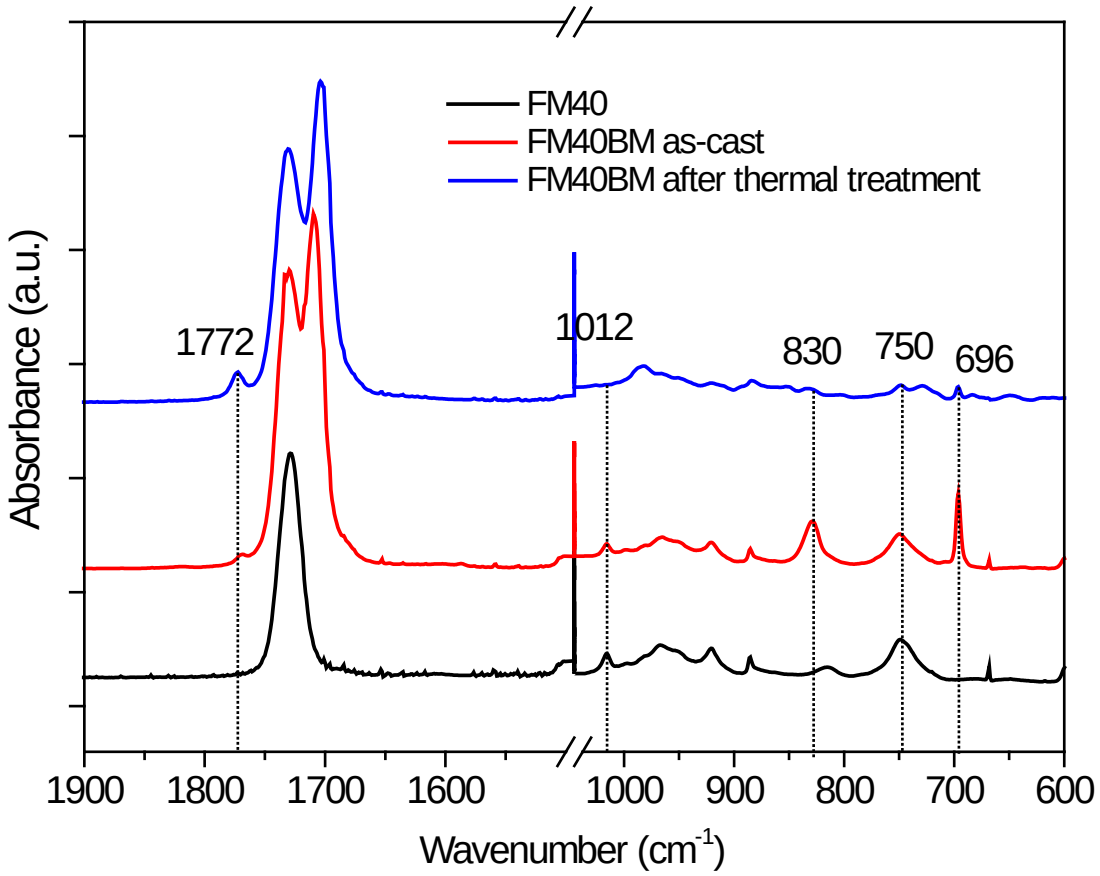

Figure 1. FTIR spectra of: furfuryl methacrylate linear copolymer FM40; mixed with DEBM bismaleimide and cast by spin coating; after thermal treatment (150 °C, 30 min and slow cooling to rt). FM40BM spectra normalized respect to band at 2959 cm^{-1} ($–CH_3$ str).

The spectrum of the as-cast acrylate/bismaleimide blend displays some characteristic peaks of the unreacted precursors: 1012 cm^{-1} and 750 cm^{-1}, ascribed to the furan ring [33, 71]; 830 cm^{-1} and 696 cm^{-1}, related to C=C stretching and C-H out-of-plane bending in maleimide rings [72], respectively. After the thermal treatment, those peaks are found to decrease in intensity and disappear, indicating successful reaction between furan and maleimide moieties (Scheme 1B). Concurrently, a new signal appears at 1772 cm^{-1}, characteristic of the formation of the DA adduct [71, 73]. Gel content experiments provided additional evidence of covalent crosslinking. Glass slides coated with the thermally treated (crosslinked) DA-based material were immersed for 24 h in THF. The solvent

caused swelling and partial detaching of the solid coating from the substrate. After filtering and solvent removal under vacuum, the insoluble content was found to be higher than 98%, indicating excellent extent of curing. Nevertheless, the peculiarity of DA-based polymer networks is the thermal reversibility of the crosslinks. This feature was conveniently checked by immersing a crosslinked sample in DMF, a good solvent for the furan precursor and the bismaleimide. The sample was insoluble at rt, while upon heating (160 °C) it was completely solubilized through r-DA decrosslinking. During slow cooling to rt (12 h), a gel phase was instead found to appear, confirming the factual reversibility of the formed crosslinks.

3.4 Thermal properties

The thermal behavior of the coatings studied through DSC measurements highlighted the effect of DA-crosslinking on the properties of furan-modified linear copolymers (Figure 2 and Table 2).

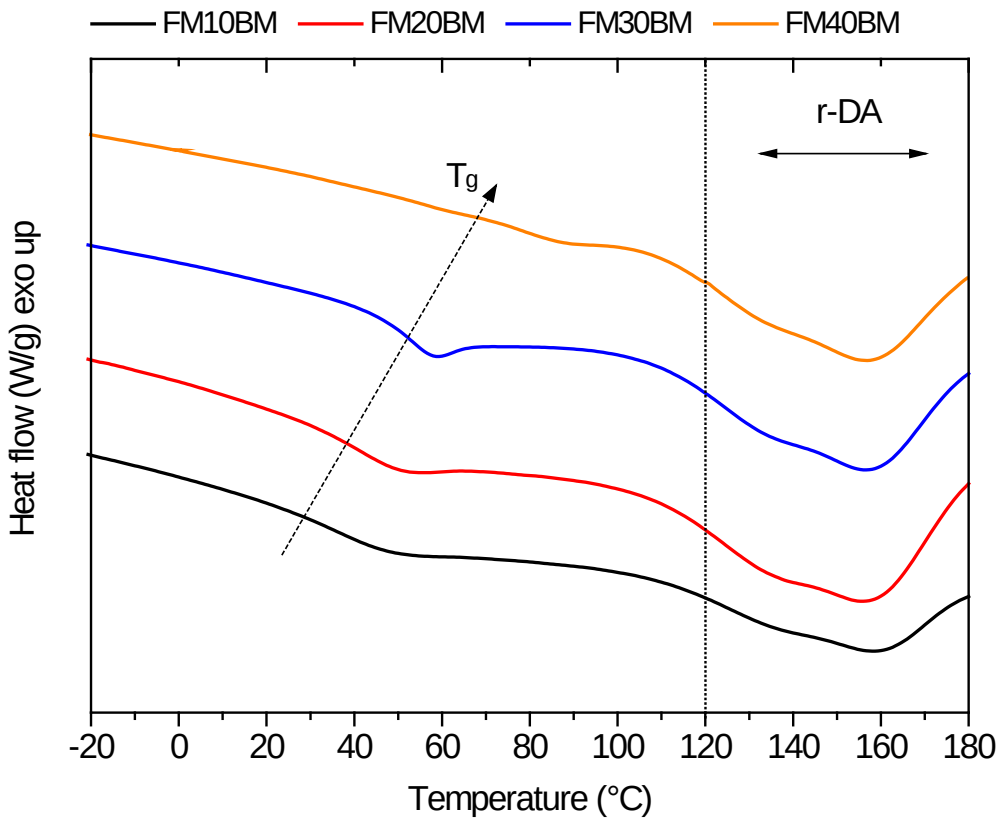

Figure 2 DSC traces (first heating scans) of all crosslinked coatings with different degree of furan functionalization.

First, a broad endotherm in the 120 –170 °C range and peaking at 156 °C was observed in each curve and indicated the scission of furan/maleimide adducts (r-DA reaction) [74], proving the thermal reversibility of the formed crosslinks. The observed temperature ranges for the r-DA process are characteristic of the furan/maleimide couple [75]. Furthermore, all crosslinked samples exhibited a single T_g, higher than their linear acrylate precursors, as expected. By increasing the functionality of the network (*i.e.* furan to maleimide molar ratio) it was possible to consistently increase its rigidity, as a result of the higher crosslinking density. All observed T_g values are above rt: in particular, *FM30BM* and *FM40BM* formulations appear suitable for application in outdoor environments being their $T_g \geq 50$ °C. TGA measurements performed in air pointed out that no significant mass loss was present below 200 °C (Table 2 and Figure S5 in the Supporting Information), particularly in the r-

DA temperature range, which is of interest for the self-healing ability. In addition, the increase of network rigidity (*viz.*, increase in T_g) was found to be beneficial for thermal stability, as reported for similar systems [31] and for crosslinked acrylates in general [76].

Table 2 Properties of FMA-*co*-EHMA polymers after crosslinking with butanediol diester bismaleimide (DEBM): thermal behavior determined from DSC; temperature for 2% mass loss ($T_{2\%}$) and for maximum degradation rate (T_{max}) from TGA in air; static contact angle measurements in water (ϑ_{H2O}), diodomethane (ϑ_{DIM}), calculated dispersive (γ_d) and polar (γ_p) component of surface energy and pull-off adhesion strength for selected coatings.

Sample	T_g [°C]	$T_{r\text{-}DA}$ [°C]	$T_{2\%}$ [°C]	T_{max} [°C]	ϑ_{H2O} [°]	ϑ_{DIM} [°]	γ_d [mN/m]	γ_p [mN/m]	*Adhesive strength* [MPa]
FM10BM	29	120-170	251	292	100.6±0.6	64.4±0.7	24.67	1.01	>8
FM20BM	38	120-170	256	294	100.0±0.6	63.2±1.7	25.30	1.04	
FM30BM	50	120-170	260	357	100.5±1.7	59.2±2.0	28.09	0.66	
FM40BM	77	120-170	258	360	101.3±0.8	58.7±1.2	28.64	0.50	>8

3.5 Optical and surface properties

All the crosslinked polymers were visually clear and homogeneous after spin coating on glass slides and thermal treatment. Indeed, transmittance values, measured through UV-Vis spectroscopy, were > 95% in the 350 – 750 nm spectral range (Figure 3), compared to a clean glass slide as a reference. Such high transparency was independent of the degree of functionality of the system and can be ascribed to the absence of light absorbing moieties in the novel aliphatic bismaleimide and the furan precursor, combined with the amorphous nature of the DA-based polymer networks [77]. In view of a potential application as optical waveguide, reflectance and refractive index were also determined. Reflectance ranged between 7.9-8.1% for all the samples, over the 400 – 750 nm spectral range, while

refractive index for selected FM20BM and FM30BM samples was 1.50, both in close agreement to values reported for standard PMMA [78]. These results evidence a possible use of these functional materials for optical applications as substitutes to PMMA.

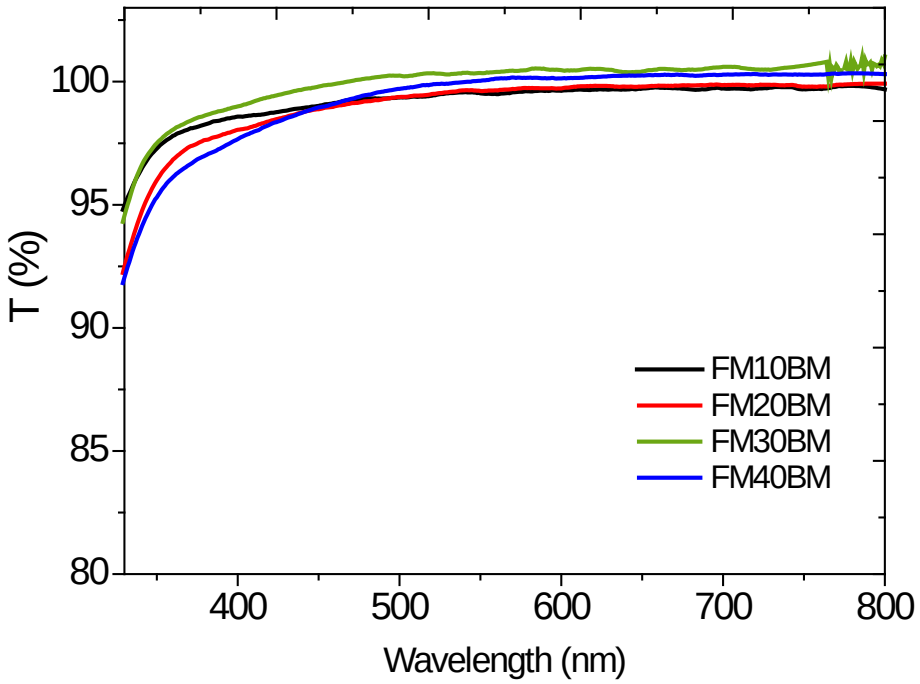

Figure 3 UV-Vis transmittance spectra of all crosslinked formulations coated on glass.

Further characterization of these coatings included the evaluation of technological properties such as wettability and adhesion strength. Static optical contact angle (OCA) measurements (Table 2) denoted the moderate hydrophobic character of the DA-crosslinked coatings with values of water contact angles ϑ_{H2O} around 100°. Surface properties were slightly affected by the presence of furan/maleimide adducts with surface energy γ values being essentially determined by the dispersive component γ_d, probably owing to the non-polar character of 2-ethylhexyl pendant groups in the copolymer. The adhesion strength was evaluated on *FM10BM* and *FM40BM*, being the formulations with the lowest and the highest T_g, respectively. Failure mode was cohesive in the coating layer for all the tests, as the coatings were not detached from the glass substrate. An average adhesion strength higher than 8 MPa was recorded on the examined materials, with no significant difference between the samples.

3.6 Self-healing assessment

The thermally triggered self-healing ability was studied on all the formulations. After the crosslinking treatment, coatings were superficially damaged with a scalpel blade, producing a scratch with a depth between 1-2 μm and width between 20-50 μm. Repair treatments were performed under different conditions of time and temperatures, between 120 and 170 °C. Each treatment was followed by a slow cooling step to rt, analogously to the coating fabrication step, and the evolution of the damage was monitored by optical microscopy. A first series of tests was performed at 120 °C, which corresponds to the onset of the endotherm transition associated to r-DA, as observed in DSC traces. While a decrease in the scratch width was observed in all the formulations, a complete repair was achieved only in *FM10BM* and *FM20BM*, the coatings with lower functional content, only after 20 h of thermal treatment. These results evidenced that material could re-flow and close the scratches at mild temperature, even though the time scale appeared too long for practical applications. When the thermal treatment was performed at 140 °C, times for complete repair were drastically reduced to 1 h and 5 h for *FM10BM* and *FM20BM*, respectively. However, only partial (or no) recovery was observed in *FM30BM* and *FM40BM* samples. At 160 °C full recovery was achieved within 1 h for all damaged samples except for *FM40BM*, which eventually required 90 min at 170 °C. Micrographs of samples healed under optimized thermal treatment time at different temperature are reported in Figure 4.

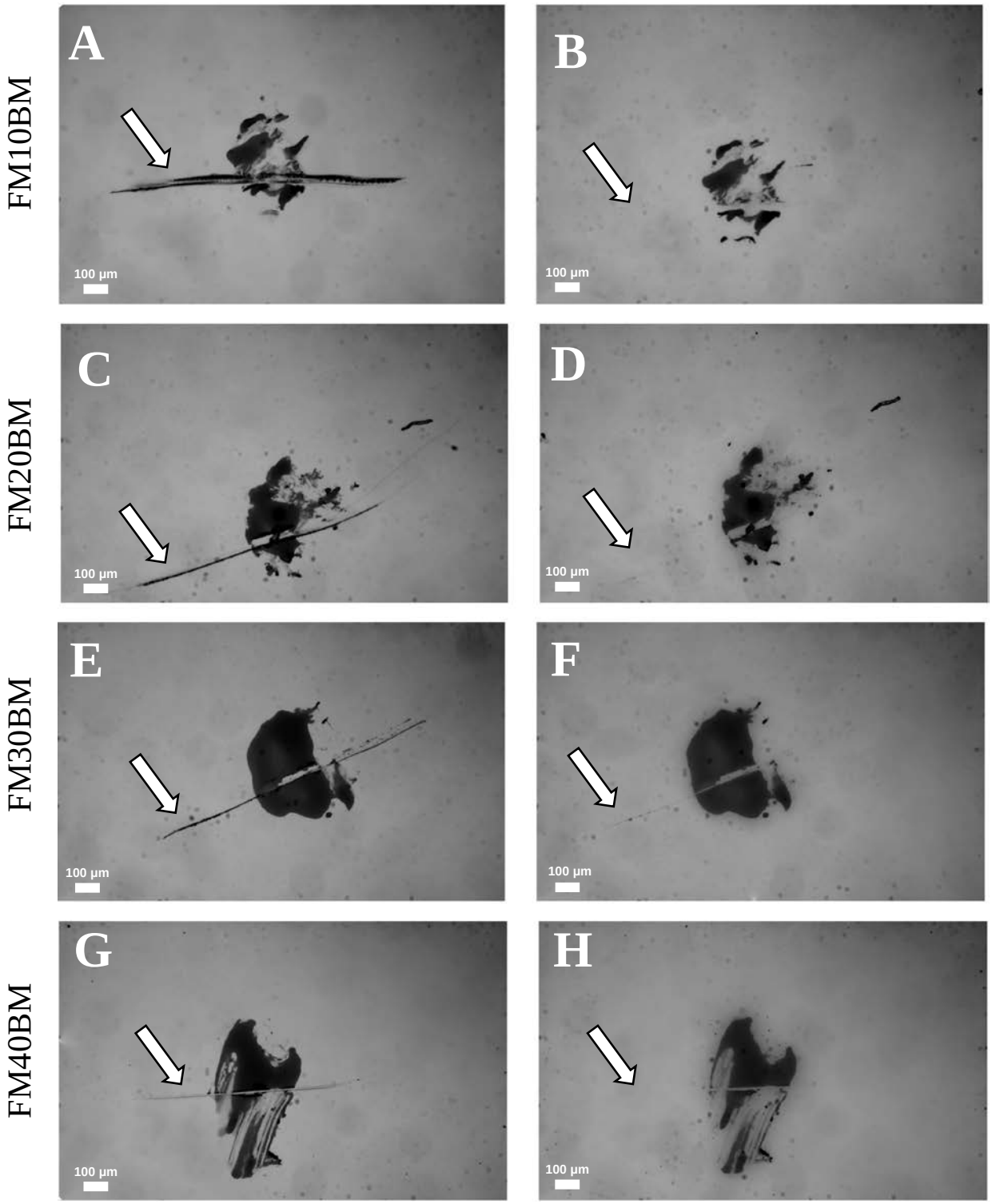

Figure 4 Optical microscope images of coating obtained from copolymers of FMA crosslinked with DEBM bismaleimide with increasing degree of functionality: (A, C, E, G) damaged by scratching with a scalpel and

healed in (B) 1 h, 140 °C (D, F) 1 h, 160 °C (H) 1.5 h, 170 °C. The white arrows indicate the damaged/mended area.

Clearly, the mobility of the networks played a key role in the healing ability, as coatings with higher T_g (higher rigidity) required increasingly longer times and/or higher temperatures to achieve full repair [34, 38]. However, it has to be noted that the observed times for repair are equal or slightly shorter than those previously reported for DA-coatings with analogous network architecture [31, 35, 40, 41], which highlights the excellent healing properties of these novel DA-based polymeric systems. In order to gauge the possibility to undergo multiple healing cycles, after the first repair treatment, some samples were scratched again in the same area and thermally annealed under the appropriately optimized conditions, namely 1 h at 140 °C or 160 °C, followed by slow cooling. The complete repair confirmed the intrinsic self-healing ability of the coatings due to dynamic DA chemistry (Figure S6 in the Supporting Information).

3.7 Optical degradation

The optical stability of the coatings was studied under the conditions required for thermal healing. A visual inspection of healed coatings after heat treatment allowed to detect yellowing, especially in the formulations with higher degree of furan functionality. In order to quantitatively assess this aspect, UV-Vis spectra of *FM40BM* (*i.e.*, the coating with the highest content of DA adducts) were recorded before and after the healing treatment (Figure 5). Indeed, a decrease of around 10% in transmittance over the near UV and violet region of the spectrum was observed, giving account of the appearance of the yellow coloration. The phenomenon was attributed to thermo-oxidative degradation of the polymer network mediated by radicals, possibly owing to the relative instability of the C-H bond in position 5 of the furfuryl ring already at moderate temperatures [79]. Based on this assumption, a new coating was formulated by including a common phenolic antioxidant (Irganox 1010) at 0.2 wt.% [80]. Compared to the pure coating, the stabilized one retained its high transmittance (> 95%) after the

thermal healing treatment (Figure 5A), owing to the radical deactivating activity of Irganox 1010. FTIR spectra recorded on the pure *FM40BM* after 1 h and 2 h of thermal treatment at 170 °C displayed a slight decrease in the intensity of the band at 1705 cm^{-1}, suggesting progressive cleavage of carbonyl groups in imide rings (Figure 5B). Based on these results, the antioxidant was included in all the formulations for the following characterizations.

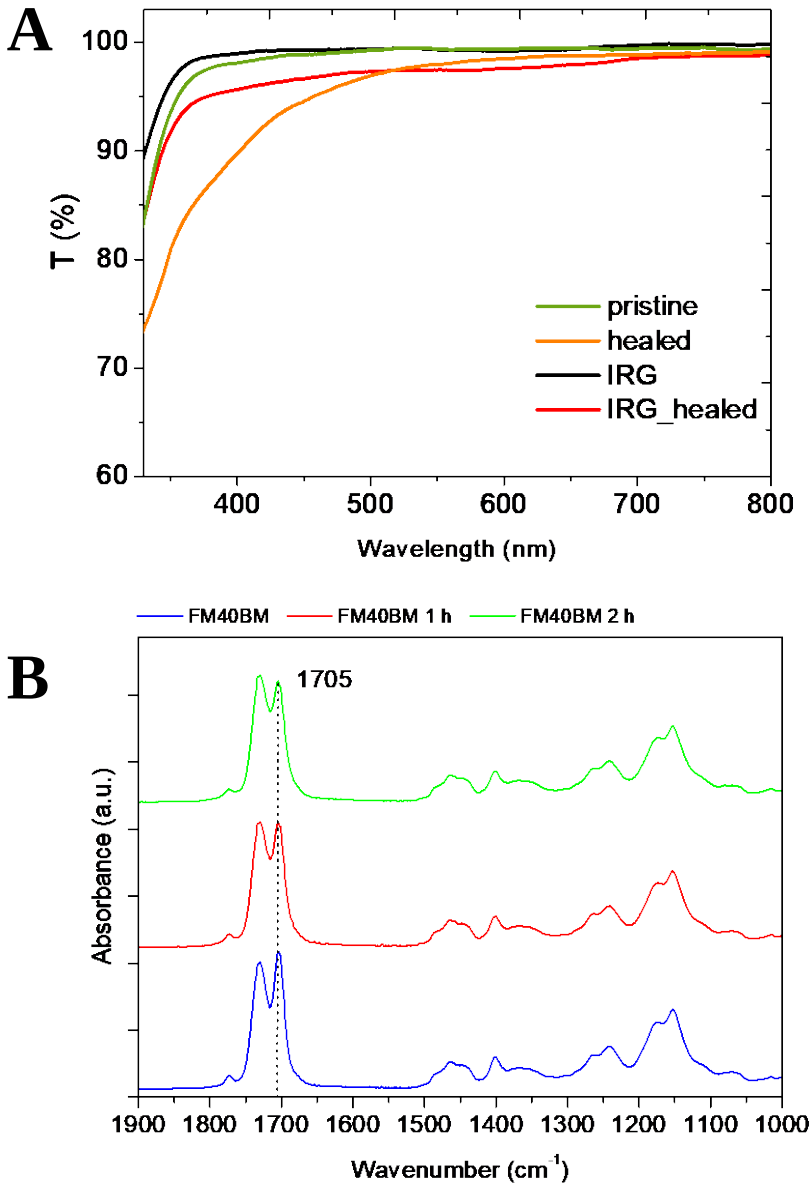

Figure 5 (A) UV-Vis spectra of pristine compared to stabilized (labelled IRG) FM40BM coating, before and after thermal treatment for healing (170 °C, 90 min); (B) FTIR spectra of neat FM40BM after healing treatment at 170 °C for 1 h and 2 h.

Accelerated weathering tests were performed in order to assess the potential suitability of these novel DA-based coatings for use in outdoor environment. *FM30BM* formulation was selected for its good compromise between sufficiently high T_g and efficient healing performance.

First, FTIR recorded after different exposure times did not evidence any relevant structural modification of the material caused by weathering (Figure S7 in the Supporting Information). Satisfactory stability was confirmed by the DA-based coatings, which displayed full retention of high transmittance in the visible region, even after 504 h of cumulative irradiation (Figure 6A). Moreover, from the functional point of view, the healing ability was unaffected by weathering, as reported in Figure 6B.

Secondly, weathering tests were conducted on pigmented coatings. To this end, titania was incorporated in the crosslinked materials, leading to white coatings, with a Hunter whiteness index (WI_H) of 85, calculated from colorimetric analysis, indicative of a light grey shade [81]. Upon irradiation, WI_H was retained and the total color difference (ΔE) over light exposure time was found to remain below the threshold value for perceptual color change (> 2.3) (Figure 6C) [82].

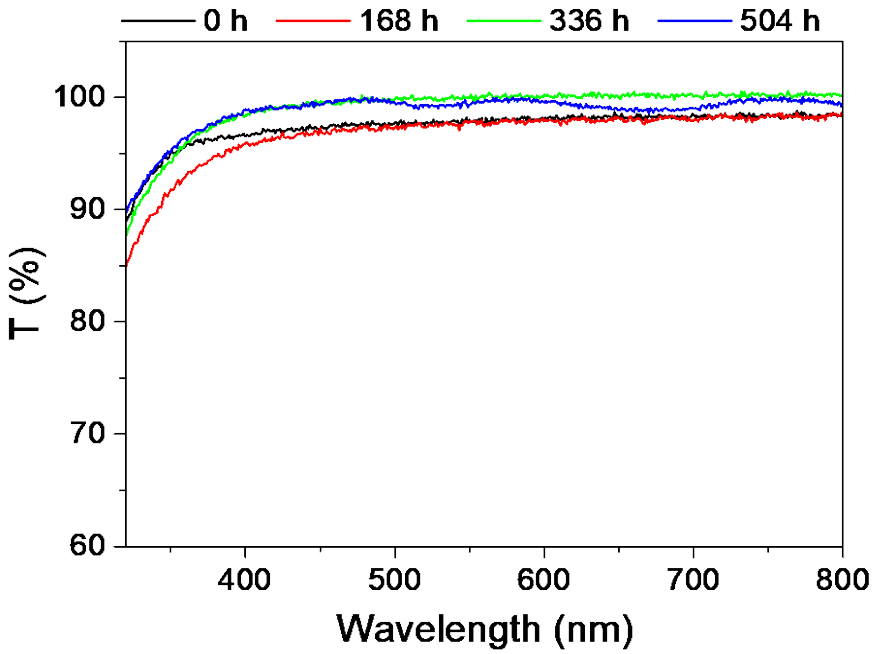
0 h
168 h
336 h
504 h
T (%)
100
90
80
70
60
400
500
600
700
800
Wavelength (nm)

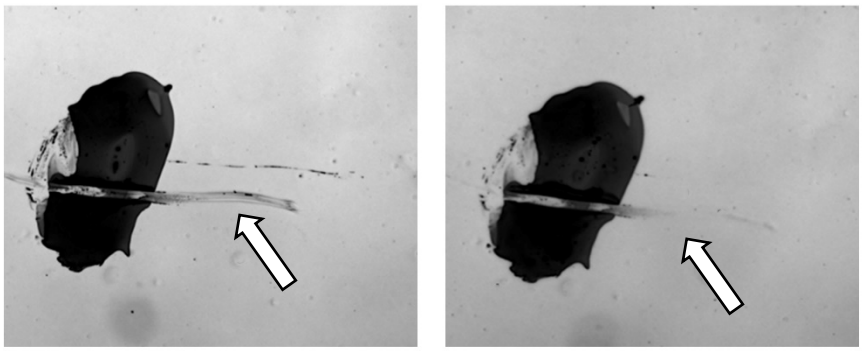

C

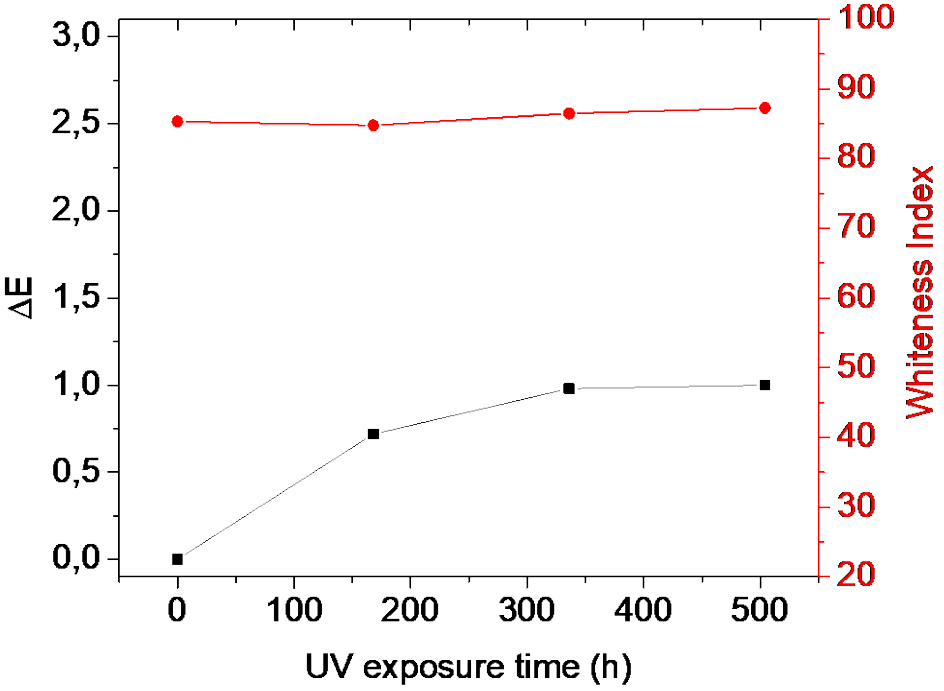
ΔE
3,0
2,5
2,0
1,5
1,0
0,5
0,0
0
100
200
300
400
500
UV exposure time (h)
Whiteness Index
100
90
80
70
60
50
40
30
20

Figure 6 Effect of weathering on: (A) Transmittance of clear FM30BM coating; (B) self-healing ability (healing cycle: 1 h at 160 °C followed by slow cooling to rt), the white arrows indicate the damaged/mended areas; (C) colorimetric parameters, namely Whiteness Index (WI_H) and total color difference (ΔE) of FM30BM coating pigmented with titania.

3.8 Properties of the nanocomposite coatings

In technological applications, surface hardness of coatings is very often sought in order to provide the underlying substrate with an additional protection to mechanical damages. To this end, nano-reinforced coatings are typically obtained by introducing nanofillers in the organic matrix, provided that they can be dispersed homogeneously into it and that they do not aggregate during coating formation [83]. In this work, a solution blending method was employed as a fast and simple way to prepare hybrid DA-based coatings starting from unmodified silica nanoparticles (scheme for sample preparation reported in Figure S8 in the Supporting Information). SiO_2 was first dispersed in the furan copolymer solution *via* ultrasonication. An ice bath was used to control the temperature rise in order to minimize solvent loss. DEBM linker was added after the sonication step, in order to avoid premature gelation due to the DA reaction. *FM20BM* and *FM30BM* formulations were selected owing to their good balance between T_g and self-healing properties.

A visual inspection of the crosslinked composite coatings evidenced that a 5 wt% loading of nano-SiO_2 caused a decrease in the coating transparency, which was confirmed by the lowering in transmittance values at 550 nm (Figure 7A and Figure S14 in the Supporting Information for transmittance in the full visible range). Loss of transparency can be attributed to phase separation of domains with size > 400 nm [84]. Conversely a good dispersion was observed in the coatings at lower silica content (1 wt% and 3 wt%), which exhibited the same high transparency as the neat polymer coatings. SEM and AFM images recorded on the sample with 3wt% loading confirmed the good dispersion, as no evidence of nanosilica aggregates was detected either on the surface or in the cross-

section of the coating (Figures S9-S12 in the Supporting Information). EDX analysis confirmed the presence of silica in the nanocomposite (Figure S13 in the Supporting Information).

DSC traces displayed 20 °C increase in T_g for both composite formulations compared to the unfilled polymer networks, but only up to a 3 wt.% filler content (Figure 7B). The shift in the T_g indicates a good polymer-filler interaction at the nanoscale, even in the absence of chemical modifications to the nanoparticles such as in this case. The r-DA endotherm transition was found in the same range of temperature as the neat polymeric coatings. Residual masses at 800 °C from TGA matched the nanosilica loading in the formulations (Table S1 in the Supporting Information).

Surface hardness evaluation of the nanocomposite coatings was performed by means of pencil hardness tests, which showed a significant reinforcement effect on the surface scratch resistance. The neat coatings are relatively soft, namely *FM30BM* has a higher grade (2B) compared to *FM20BM* (3B) owing to its higher functionality. Upon addition of a small amount of nanofiller, hardness is significantly enhanced, up to F and B grades for *FM30BM* and *FM20BM* respectively (Figure 7C), which are in the range of surface hardness of common polycarbonate [85].

From a functional point of view, the nanocomposites substantially preserved the self-healing ability observed for the neat DA matrix as evidenced in the optical micrographs (Figure 8) as well as in the SEM and AFM images (Figures S15-17 in the Supporting Information). Despite the diminished chain mobility resulting from the introduction of the inorganic nanofiller, effective repair of small scratches was observed even at higher silica loading (3 and 5 wt%) after 1 h of thermal treatment at 160 °C. Interestingly, the composite coatings with 1 wt.% of nanosilica displayed full scratch repair under the same conditions, similarly to their (unfilled) pristine matrices, while having comparatively higher T_g values, namely 53 °C for *FM20BM* and 61 °C for *FM30BM*.

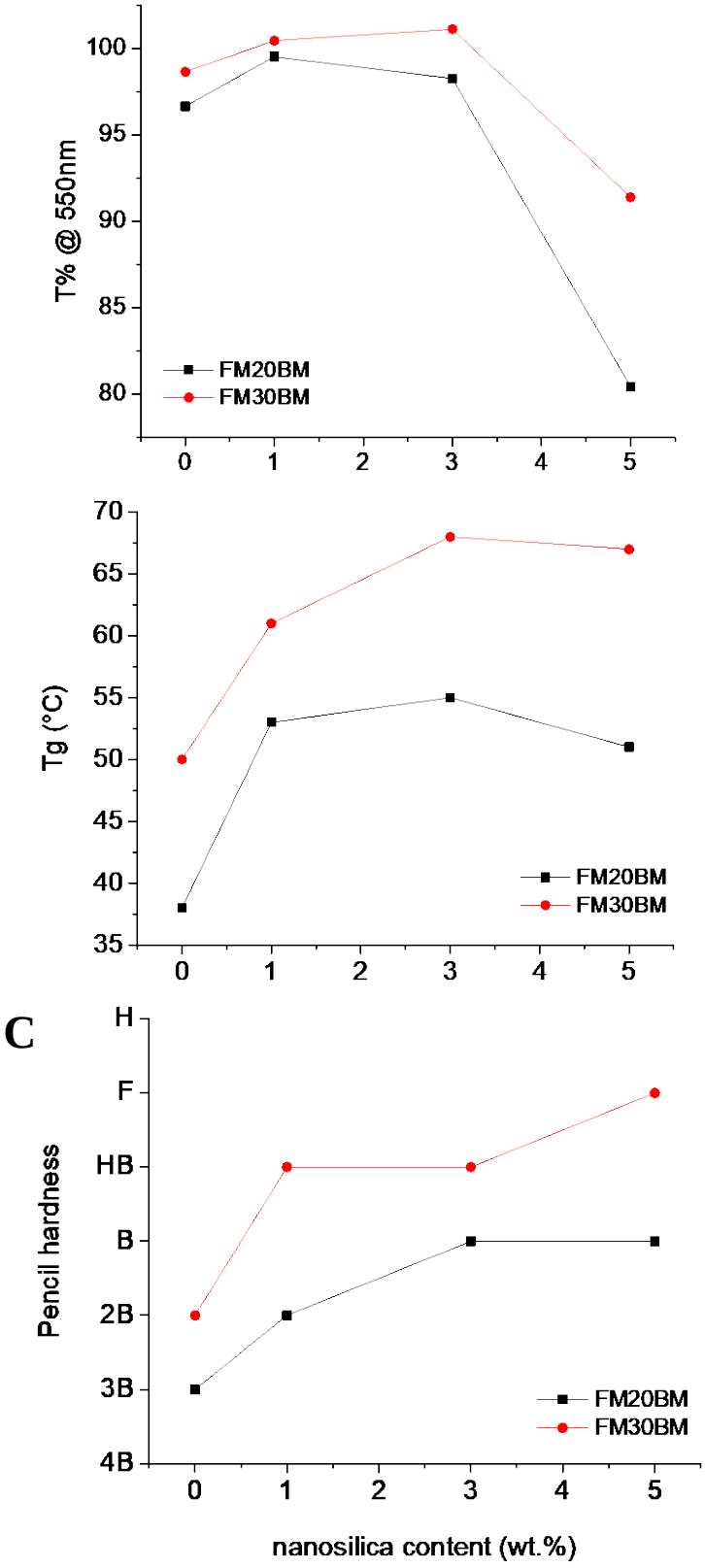

Figure 7 Properties of nanocomposites as a function of nano-SiO_2 content: (A) transmittance measured at 550 nm; (B) T_g from DSC analysis; (C) pencil hardness values.

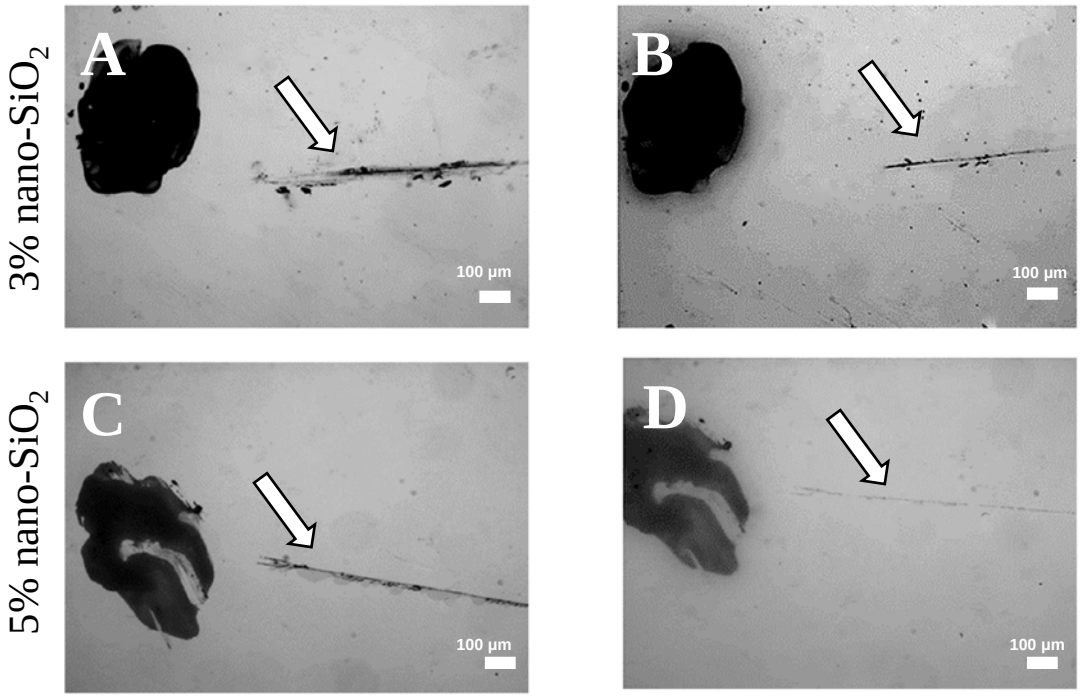

Figure 8 Self-healing assessment of composite coatings based on FM30BM with different amounts of nano-SiO_2: (A, C) damaged; (B, D) after thermal treatment at 160 °C for 1 h. The white arrows indicate the damaged/mended areas.

4 Conclusions

In conclusion, novel thermo-responsive polymer networks characterized by high transparency, prolonged durability and excellent self-healing response were presented in this work.

A series of linear copolymers of furfuryl methacrylate and 2-ethylexyl methacrylate were synthetized *via* free radical polymerization and crosslinked with a novel, amorphous and highly soluble aliphatic bismaleimide obtained from a biobased precursor in one step and reported here for the first time.

The rigidity/mobility of the DA-based crosslinked polymer networks was tuned by systematically varying the furan and maleimide content, resulting in networks with T_g values ranging from 28 to 77 °C. All of them were found to exhibit excellent thermo-responsiveness, as assessed by DSC analysis, and were able to efficiently repair superficial scratches by applying appropriately optimized mild

temperature treatments (120 – 170 °C) according to their functionality. Rising the thermal treatment temperature ensured a significant reduction in the time required for complete scratch repair.

All the coatings were highly transparent and colorless. These two properties were essentially unaffected by the self-healing thermal treatment and upon accelerated weathering, after proper addition of a conventional phenolic antioxidant, thus demonstrating the high robustness of the presented materials in terms of prolonged outdoor durability. Self-healing ability was preserved after weathering and was observed also in titania-pigmented coatings. Finally, a significantly enhanced surface hardness was obtained in DA-based nanocomposite coatings even in the presence of low amounts of silica nanoparticles used as inorganic reinforcing filler.

In light of the above considerations, the presented polymer network combines the well-known versatility and easy application of acrylic polymers, with the possibility to repair the coating by a moderate thermal treatment. The wide range of attainable glass transition temperatures, obtained by simply tuning the DA functionality, suggests applications ranging from adhesives to floor care coatings [81]. Within this context, the excellent transparency and the possibility to incorporate pigmented fillers, indicate the application as binder for decorative paints. In addition, similar to acrylics, transparency is retained upon weathering tests and thermal cycles in the presence of a general-purpose stabilizer. This feature, paired with the possibility to enhance the scratch resistance by incorporation of silica nanofillers, pave the way to the use of these materials as protective coatings in outdoor environment. This study provides the first example of highly durable, transparent and self-healable coatings based on the combination of a novel aliphatic bismaleimide and different furan-functionalized polyacrylate copolymers. The systematic investigation of the structure-property relationships of these materials gives important guidelines for the design of thermo-responsive DA polymer networks of controlled thermal, optical, surface and functional characteristics, in view of their potential use in the field of advanced industrial protective coatings.

5 Acknowledgements

The authors greatly acknowledge Gigliola Clerici for her kind support with thermal and GPC analyses.

6 Data availability

The raw/processed data required to reproduce these findings cannot be shared at this time as the data also forms part of an ongoing study.

7 References

[1] M.F. Montemor, Functional and smart coatings for corrosion protection: A review of recent advances, Surf. Coat. Technol., 258 (2014) 17-37.
[2] F. Zhang, P.F. Ju, M.Q. Pan, D.W. Zhang, Y. Huang, G.L. Li, X.G. Li, Self-healing mechanisms in smart protective coatings: A review, Corros. Sci., 144 (2018) 74-88.
[3] M.D. Hager, P. Greil, C. Leyens, S. van der Zwaag, U.S. Schubert, Self-Healing Materials, Adv. Mater., 22 (2010) 5424-5430.
[4] W.H. Binder, Self-Healing Polymers: From Principles to Applications, Wiley, 2013.
[5] Y. Yang, M.W. Urban, Self-healing polymeric materials, Chem. Soc. Rev., 42 (2013) 7446-7467.
[6] D.G. Bekas, K. Tsirka, D. Baltzis, A.S. Paipetis, Self-healing materials: A review of advances in materials, evaluation, characterization and monitoring techniques, Compos. Part B Eng., 87 (2016) 92-119.
[7] M.D. Hager, S. van der Zwaag, U.S. Schubert, Self-healing Materials, Springer International Publishing, 2016.
[8] S.J. Garcia, Effect of polymer architecture on the intrinsic self-healing character of polymers, Eur. Polym. J., 53 (2014) 118-125.
[9] F. García, M.M.J. Smulders, Dynamic covalent polymers, J. Polym. Sci. A Polym. Chem., 54 (2016) 3551-3577.
[10] S. Billiet, X.K.D. Hillewaere, R.F.A. Teixeira, F.E. Du Prez, Chemistry of Crosslinking Processes for Self-Healing Polymers, Macromol. Rapid Commun., 34 (2013) 290-309.
[11] W. Zou, J. Dong, Y. Luo, Q. Zhao, T. Xie, Dynamic Covalent Polymer Networks: from Old Chemistry to Modern Day Innovations, Adv. Mater., 29 (2017) 1606100.
[12] J.M. Winne, L. Leibler, F.E. Du Prez, Dynamic covalent chemistry in polymer networks: a mechanistic perspective, Polym. Chem., (2019).
[13] N. Kuhl, S. Bode, M.D. Hager, U.S. Schubert, Self-Healing Polymers Based on Reversible Covalent Bonds, in: M.D. Hager, S. VanDerZwaag, U.S. Schubert (Eds.) Self-Healing Materials, 2016, pp. 1-58.
[14] O. Diels, K. Alder, Synthesen in der hydroaromatischen Reihe, Justus Liebig's Annalen der Chemie, 460 (1928) 98-122.
[15] J.M. Craven, Cross-linked thermally reversible polymers produced from condensation polymers with pendant furan groups cross-linked with maleimides, US3435003A (1969).
[16] X. Chen, F. Wudl, A.K. Mal, H. Shen, S.R. Nutt, New Thermally Remendable Highly Cross-Linked Polymeric Materials, Macromolecules, 36 (2003) 1802-1807.
[17] Z. Karami, M.J. Zohuriaan-Mehr, A. Rostami, Biobased Diels-Alder engineered network from furfuryl alcohol and epoxy resin: Preparation and mechano-physical characteristics, ChemistrySelect, 3 (2018) 40-46.

[18] Ž. Štirn, A. Ručigaj, J. Karger-Kocsis, M. Krajnc, Effects of Diels–Alder Adduct and Lass Transition on the Repeated Self-Healing of Aliphatic Amine-Cured Epoxy Resin, Macromol. Mater. Eng., 303 (2018).
[19] H.W. Zhao, L.B. Feng, X.T. Shi, Y.P. Wang, Y.H. Liu, Synthesis and healing behavior of thermo-reversible self-healing epoxy resins, Acta Polym. Sinica, (2018) 395-401.
[20] G. Fortunato, L. Anghileri, G. Griffini, S. Turri, Simultaneous Recovery of Matrix and Fiber in Carbon Reinforced Composites through a Diels-Alder Solvolysis Process, Polymers, 11 (2019).
[21] Y.L. Fang, X.S. Du, S.W. Yang, H.B. Wang, X. Cheng, Z.L. Du, Sustainable and tough polyurethane films with self-healability and flame retardance enabled by reversible chemistry and cyclotriphosphazene, Polym. Chem., 10 (2019) 4142-4153.
[22] A.V. Menon, G. Madras, S. Bose, The journey of self-healing and shape memory polyurethanes from bench to translational research, Polym. Chem., 10 (2019) 4370-4388.
[23] K.K. Tremblay-Parrado, L. Averous, Renewable Responsive Systems Based on Original Click and Polyurethane Cross-Linked Architectures with Advanced Properties, ChemSusChem, (2019).
[24] P. Tanasi, M.H. Santana, J. Carretero-Gonzalez, R. Verdejo, M.A. Lopez-Manchado, Thermo-reversible crosslinked natural rubber: A Diels-Alder route for reuse and self-healing properties in elastomers, Polymer, 175 (2019) 15-24.
[25] J.K. Wang, C. Lv, Z.X. Li, J.P. Zheng, Facile Preparation of Polydimethylsiloxane Elastomer with Self-Healing Property and Remoldability Based on Diels-Alder Chemistry, Macromol. Mater. Eng., 303 (2018).
[26] L.M. Polgar, G. Fortunato, R. Araya-Hermosilla, M. van Duin, A. Pucci, F. Picchioni, Cross-linking of rubber in the presence of multi-functional cross-linking aids via thermoreversible Diels-Alder chemistry, Eur. Polym. J., 82 (2016) 208-219.
[27] R. Araya-Hermosilla, G. Fortunato, A. Pucci, P. Raffa, L. Polgar, A.A. Broekhuis, P. Pourhossein, G.M.R. Lima, M. Beljaars, F. Picchioni, Thermally reversible rubber-toughened thermoset networks via Diels–Alder chemistry, Eur. Polym. J., 74 (2016) 229-240.
[28] F. Picchioni, A. Broekhuis, Y. Zhang, Thermally Self-Healing Polymeric Materials: The Next Step to Recycling Thermoset Polymers?, Macromolecules, 42 (2009).
[29] M.B. Banella, G. Giacobazzi, M. Vannini, P. Marchese, M. Colonna, A. Celli, A. Gandini, C. Gioia, A Novel Approach for the Synthesis of Thermo-Responsive Co-Polyesters Incorporating Reversible Diels-Alder Adducts, Macromol. Chem. Phys., 220 (2019).
[30] M. Bednarek, P. Kubisa, Reversible networks of degradable polyesters containing weak covalent bonds, Polym. Chem., 10 (2019) 1848-1872.
[31] A.A. Kavitha, N.K. Singha, “Click Chemistry” in Tailor-Made Polymethacrylates Bearing Reactive Furfuryl Functionality: A New Class of Self-Healing Polymeric Material, ACS Appl. Mater. Int., 1 (2009) 1427-1436.
[32] M. Wouters, E. Craenmehr, K. Tempelaars, H. Fischer, N. Stroeks, J. van Zanten, Preparation and properties of a novel remendable coating concept, Prog. Org. Coat., 64 (2009) 156-162.
[33] A.A. Kavitha, N.K. Singha, Smart “All Acrylate” ABA Triblock Copolymer Bearing Reactive Functionality via Atom Transfer Radical Polymerization (ATRP): Demonstration of a “Click Reaction” in Thermoreversible Property, Macromolecules, 43 (2010) 3193-3205.
[34] J. Kötteritzsch, S. Stumpf, S. Hoeppener, J. Vitz, M.D. Hager, U.S. Schubert, One-component intrinsic self-healing coatings based on reversible crosslinking by diels-alder cycloadditions, Macromol. Chem. Phys., 214 (2013) 1636-1649.
[35] N.B. Pramanik, D.S. Bag, S. Alam, G.B. Nando, N.K. Singha, Thermally amendable tailor-made functional polymer by RAFT polymerization and "click reaction", J. Polym. Sci. A Polym. Chem., 51 (2013) 3365-3374.
[36] R.K. Bose, J. Kötteritzsch, S.J. Garcia, M.D. Hager, U.S. Schubert, S. van der Zwaag, A rheological and spectroscopic study on the kinetics of self-healing in a single-component diels–alder copolymer and its underlying chemical reaction, J. Polym. Sci. A Polym. Chem., 52 (2014) 1669-1675.

[37] T. Engel, G. Kickelbick, Self-healing nanocomposites from silica − polymer core − shell nanoparticles, Polym. Int., 63 (2014) 915-923.
[38] J. Kötteritzsch, M.D. Hager, U.S. Schubert, Tuning the self-healing behavior of one-component intrinsic polymers, Polymer, 69 (2015) 321-329.
[39] S. Moon, J. Shin, S.H. Cha, Y. Shin, K.J. Lee, Introduction of reversible crosslinker into artificial marbles toward chemical recyclability, J. Ind. Eng. Chem., 31 (2015) 86-90.
[40] S. Jung, J.T. Liu, S.H. Hong, D. Arunbabu, S.M. Noh, J.K. Oh, A new reactive polymethacrylate bearing pendant furfuryl groups: Synthesis, thermoreversible reactions, and self-healing, Polymer, 109 (2017) 58-65.
[41] S.Y. Kim, T.H. Lee, Y.I. Park, J.H. Nam, S.M. Noh, I.W. Cheong, J.C. Kim, Influence of material properties on scratch-healing performance of polyacrylate-graft-polyurethane network that undergo thermally reversible crosslinking, Polymer, 128 (2017) 135-146.
[42] S.S. Patil, A. Torris, P.P. Wadgaonkar, Healable network polymers bearing flexible poly(lauryl methacrylate) chains via thermo-reversible furan-maleimide diels–alder reaction, J. Polym. Sci. A Polym. Chem., 55 (2017) 2700-2712.
[43] N.B. Pramanik, P. Mondal, R. Mukherjee, N.K. Singha, A new class of self-healable hydrophobic materials based on ABA triblock copolymer via RAFT polymerization and Diels-Alder "click chemistry", Polymer, 119 (2017) 195-205.
[44] A.K. Padhan, D. Mandal, Thermo-reversible self-healing in a fluorous crosslinked copolymer, Polym. Chem., 9 (2018) 3248-3261.
[45] Z. Tang, X. Lyu, A. Xiao, Z. Shen, X. Fan, High-Performance Double-Network Ion Gels with Fast Thermal Healing Capability via Dynamic Covalent Bonds, Chem. Mater., 30 (2018) 7752-7759.
[46] S. Banerjee, B.V. Tawade, B. Ameduri, Functional fluorinated polymer materials and preliminary self-healing behavior, Polym. Chem., 10 (2019) 1993-1997.
[47] S. Sung, S.Y. Kim, T.H. Lee, G. Favaro, Y.I. Park, S.H. Lee, J.B. Ahn, S.M. Noh, J.C. Kim, Thermally reversible polymer networks for scratch resistance and scratch healing in automotive clear coats, Prog. Org. Coat., 127 (2019) 37-44.
[48] R. Gheneim, C. Perez-Berumen, A. Gandini, Diels-Alder reactions with novel polymeric dienes and dienophiles: Synthesis of reversibly cross-linked elastomers, Macromolecules, 35 (2002) 7246-7253.
[49] G. Fortunato, E. Tatsi, B. Rigatelli, S. Turri, G. Griffini, Highly Transparent and Colorless Self-Healing Polyacrylate Coatings Based on Diels–Alder Chemistry, Macromol. Mater. Eng., 305 (2020) 1900652.
[50] Y. Zare, K.Y. Rhee, The effective conductivity of polymer carbon nanotubes (CNT) nanocomposites, J. Phys. Chem. Solids, 131 (2019) 15-21.
[51] M. Joulaei, K. Hedayati, D. Ghanbari, Investigation of magnetic, mechanical and flame retardant properties of polymeric nanocomposites: Green synthesis of MgFe2O4 by lime and orange extracts, Compos. Part B Eng., 176 (2019) 107345.
[52] Y. Zare, K.Y. Rhee, Following the morphological and thermal properties of PLA/PEO blends containing carbon nanotubes (CNTs) during hydrolytic degradation, Compos. Part B Eng., 175 (2019).
[53] Y. Zare, K.Y. Rhee, Evaluation of the Tensile Strength in Carbon Nanotube-Reinforced Nanocomposites Using the Expanded Takayanagi Model, JOM, 71 (2019) 3980-3988.
[54] Y. Zare, K.Y. Rhee, S.J. Park, A modeling methodology to investigate the effect of interfacial adhesion on the yield strength of MMT reinforced nanocomposites, J. Ind. Eng. Chem., 69 (2019) 331-337.
[55] P. Nguyen Tri, T.A. Nguyen, S. Rtimi, C.M. Ouellet Plamondon, Chapter 1 - Nanomaterials-based coatings: an introduction, in: P. Nguyen Tri, S. Rtimi, C.M. Ouellet Plamondon (Eds.) Nanomaterials-Based Coatings, Elsevier, 2019, pp. 1-7.

[56] J. Loste, J.-M. Lopez-Cuesta, L. Billon, H. Garay, M. Save, Transparent polymer nanocomposites: An overview on their synthesis and advanced properties, Prog. Polym. Sci., 89 (2019) 133-158.
[57] W. Wildner, D. Drummer, Nanofiller materials for transparent polymer composites: Influences on the properties and on the transparency—A review, J. Thermoplast. Compos. Mater., 32 (2018) 1547-1565.
[58] T. Ribeiro, C. Baleizao, J.P.S. Farinha, Functional Films from Silica/Polymer Nanoparticles, Materials, 7 (2014) 3881-3900.
[59] K. Arai, T. Mizutani, M. Miyamoto, Y. Kimura, T. Aoki, Colloidal silica bearing thin polyacrylate coat: A facile inorganic modifier of acrylic emulsions for fabricating hybrid films with least aggregation of silica nanoparticles, Prog. Org. Coat., 128 (2019) 11-20.
[60] A. Gharieh, A. Mirmohseni, M. Khorasani, Preparation of UV-opaque, Vis-transparent acrylic-silica nanocomposite coating with promising physico-mechanical properties via miniemulsion polymerization, J. Coat. Technol. Res., 16 (2019) 781-789.
[61] Y.Q. Li, L. Zhang, C.Z. Li, Highly transparent and scratch resistant polysiloxane coatings containing silica nanoparticles, J. Colloid Interface Sci., 559 (2020) 273-281.
[62] Z.Z. Lu, L.J. Xu, Y. He, J.T. Zhou, One-step facile route to fabricate functionalized nano-silica and silicone sealant based transparent superhydrophobic coating, Thin Solid Films, 692 (2019).
[63] H. Zheng, M.W. Pan, J. Wen, J.F. Yuan, L. Zhu, H.F. Yu, Robust, Transparent, and Superhydrophobic Coating Fabricated with Waterborne Polyurethane and Inorganic Nanoparticle Composites, Ind. Eng. Chem. Res., 58 (2019) 8050-8060.
[64] G. Wyszecki, W.S. Stiles, Color Science: Concepts and Methods, Quantitative Data and Formulae, 2nd Edition, 2000.
[65] D.K. Owens, R.C. Wendt, Estimation of the surface free energy of polymers, J. Appl. Polym. Sci., 13 (1969) 1741-1747.
[66] A. International, ASTM D3363-05 (2011)-Standard Test Method for Film Hardness by Pencil Test, in, ASTM International West Conshohocken, 2011.
[67] G. Kossmehl, H.-I. Nagel, A. Pahl, Cross-linking reactions on polyamides by bis- and tris(maleimide)s, Angew. Makromol. Chem., 227 (1995) 139-157.
[68] L.M. Polgar, R.J. Cerpentier Robin, H. Vermeij Gijs, F. Picchioni, v. Duin Martin, Influence of the chemical structure of cross-linking agents on properties of thermally reversible networks, Pure Appl. Chem., 88 (2016) 1103.
[69] E. Tatsi, G. Fortunato, B. Rigatelli, G. Lyu, S. Turri, R.C. Evans, G. Griffini, Thermoresponsive Host Polymer Matrix for Self-Healing Luminescent Solar Concentrators, ACS Appl. Energy Mater., 3 (2020) 1152-1160.
[70] M. Wouters, M. Burghoorn, B. Ingenhut, K. Timmer, C. Rentrop, T. Bots, G. Oosterhuis, H. Fischer, Tuneable adhesion through novel binder technologies, Prog. Org. Coat., 72 (2011) 152-158.
[71] J. Wang, C. Lv, Z. Li, J. Zheng, Facile Preparation of Polydimethylsiloxane Elastomer with Self-Healing Property and Remoldability Based on Diels-Alder Chemistry, Macromol. Mater. Eng., 303 (2018) 1800089.
[72] S. Ramesh, A. Sivasamy, J.-H. Kim, Synthesis and characterization of maleimide-functionalized polystyrene-SiO2/TiO2 hybrid nanocomposites by sol–gel process, Nanoscale Research Letters, 7 (2012) 350.
[73] K. Moazzen, M.J. Zohuriaan-Mehr, R. Jahanmardi, K. Kabiri, Toward poly(furfuryl alcohol) applications diversification: Novel self-healing network and toughening epoxy–novolac resin, J. Appl. Polym. Sci., 135 (2018).
[74] G. Scheltjens, J. Brancart, I. De Graeve, B. Van Mele, H. Terryn, G. Van Assche, Self-healing property characterization of reversible thermoset coatings, J. Therm. Anal. Calorim., 105 (2011) 805-809.
[75] A. Gandini, The furan/maleimide Diels-Alder reaction: A versatile click-unclick tool in macromolecular synthesis, Prog. Polym. Sci., 38 (2013) 1.

[76] V.V. Krongauz, Crosslink density dependence of polymer degradation kinetics: Photocrosslinked acrylates, Thermochim. Acta, 503-504 (2010) 70-84.
[77] K. Minami, Optical Plastics, in: S. Bäumer (Ed.) Handbook of Plastic Optics, Wiley-VCH, 2005, pp. 109-147.
[78] G. Griffini, Host Matrix Materials for Luminescent Solar Concentrators: Recent Achievements and Forthcoming Challenges, Frontiers in Materials, 6 (2019).
[79] C. Peniche, D. Zaldívar, A. Bulay, J.S. Román, Study of the thermal degradation of poly(furfuryl methacrylate) by thermogravimetry, Polym. Degrad. Stab., 40 (1993) 287-295.
[80] S. Nawaz, H. Hillborg, M.S. Hedenqvist, U.W. Gedde, Migration of a phenolic antioxidant from aluminium oxide-poly(ethylene-co-butyl acrylate) nanocomposites in aqueous media, Polym. Degrad. Stab., 98 (2013) 475-480.
[81] A.K.R. Choudhury, Instrumental measures of whiteness, in: A.K.R. Choudhury (Ed.) Principles of Colour and Appearance Measurement, Woodhead Publishing, 2014, pp. 344-374.
[82] G. Sharma, R. Bala, Digital Color Imaging Handbook, CRC Press, 2017.
[83] M. Sangermano, M. Messori, Scratch Resistance Enhancement of Polymer Coatings, Macromol. Mater. Eng., 295 (2010) 603-612.
[84] M. Sangermano, G. Malucelli, E. Amerio, A. Priola, E. Billi, G. Rizza, Photopolymerization of epoxy coatings containing silica nanoparticles, Prog. Org. Coat., 54 (2005) 134-138.
[85] E. Chwa, L. Wu, Z. Chen, Factors towards Pencil Scratch Resistance of Protective Sol-Gel Coatings on Polycarbonate Substrate, Key Eng. Mater., 312 (2006) 339-344.